Biochemical and Biophysical Research Communications 450 (2014) 723–728

Contents lists available at ScienceDirect

Biochemical and Biophysical Research Communications

journal homepage: www.elsevier.com/locate/ybbrc

Continuous wave W- and D-Band EPR spectroscopy offer "sweet-spots" for characterizing conformational changes and dynamics in intrinsically disordered proteins

Thomas M. Casey, Zhanglong Liu, Jackie M. Esquiaqui, Natasha L. Pirman [1], Eugene Milshteyn [2], Gail E. Fanucci *

Department of Chemistry, University of Florida, PO Box 117200, Gainesville, FL 32611, USA

ARTICLE INFO

Article history:
Received 5 June 2014
Available online 17 June 2014

Keywords:
Intrinsically disordered proteins
Site-directed spin-labeling
EPR spectroscopy
Multi-frequency EPR
High-field EPR

ABSTRACT

Site-directed spin labeling (SDSL) electron paramagnetic resonance (EPR) spectroscopy is a powerful tool for characterizing conformational sampling and dynamics in biological macromolecules. Here we demonstrate that nitroxide spectra collected at frequencies higher than X-band (~9.5 GHz) have sensitivity to the timescale of motion sampled by highly dynamic intrinsically disordered proteins (IDPs). The 68 amino acid protein IA_3, was spin-labeled at two distinct sites and a comparison of X-band, Q-band (35 GHz) and W-band (95 GHz) spectra are shown for this protein as it undergoes the helical transition chemically induced by tri-fluoroethanol. Experimental spectra at W-band showed pronounced line shape dispersion corresponding to a change in correlation time from ~0.3 ns (unstructured) to ~0.6 ns (α-helical) as indicated by comparison with simulations. Experimental and simulated spectra at X- and Q-bands showed minimal dispersion over this range, illustrating the utility of SDSL EPR at higher frequencies for characterizing structural transitions and dynamics in IDPs.

1. Introduction

Site-directed spin labeling (SDSL) electron paramagnetic resonance (EPR) spectroscopy is a popular method for characterizing dynamic motions and conformational changes in biological macromolecules [1–8]. In this method, a persistent nitroxide radical is site-specifically incorporated within macromolecules at a position where there is particular interest in dynamical behavior. The continuous wave (CW) EPR nitroxide spectrum reflects motional averaging of the g tensor as well as the ^{14}N hyperfine coupling tensor due to dynamic motions of the spin label. One way to describe the motions is with a rotational correlation time; the time over which a combination of the overall tumbling of the macromolecule (τ_r), characteristic backbone motions where the spin label is attached (τ_B), and internal modes of motion of the spin label itself (τ_i), are completely sampled [3,8].

For globular proteins >15 kD and membrane bound proteins at ambient temperatures, the line shapes in the CW EPR nitroxide spectra are typically dominated by the effects of τ_B and τ_i. Plots of empirical line shape parameters, such as the second moment ($\langle H^2 \rangle$) and central line width (ΔH_0), provide a simple visual means for describing the relative line shapes associated with various structured regions of proteins such as buried sites, tertiary contacts, loops, or unstructured regions [1,8–10]. Fig. 1 demonstrates relationships between the inverse second moment, $\langle H^2 \rangle^{-1}$, and inverse central line width, ΔH_0^{-1}, of X-band (9.5 GHz) CW EPR nitroxide spectra for these distinct structured regions. Spin labels with slower motions; *i.e.*, longer correlation times, have increasingly broadened spectra owed to incomplete averaging of the g and ^{14}N hyperfine tensors on the time scale of the X-band experiment. For example, spin labels in buried sites typically lead to values for $\langle H^2 \rangle^{-1}$ and ΔH_0^{-1} that cluster in the lower left hand corner of this inverse plot and correspond to correlation times near 10 ns [7,9,11]. On the other hand, spin-labels located in flexible loops typically display correlation times near 1 ns, giving values for $\langle H^2 \rangle^{-1}$ and ΔH_0^{-1} that appear in the upper right hand corner of the inverse plot.

In cases where nitroxide spin labels are attached to smaller globular proteins, unstructured proteins or protein regions [9,12–18],

* Corresponding author. Fax: +1 352 392 0872.
E-mail address: fanucci@chem.ufl.edu (G.E. Fanucci).
[1] Current address: Department of Cellular & Molecular Physiology, Yale University, West Haven, CT 06516, USA.
[2] Current address: Department of Radiology and Biomedical Imaging, University of California, San Francisco, CA, USA.

http://dx.doi.org/10.1016/j.bbrc.2014.06.045
0006-291X/

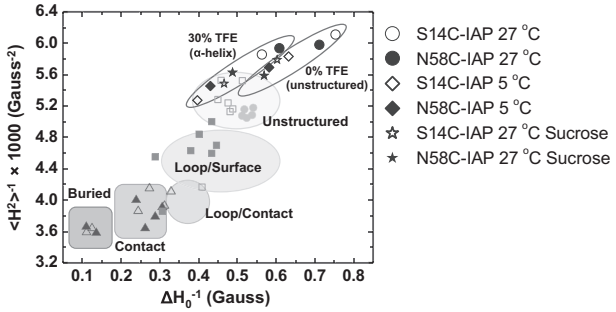

Fig. 1. Plot of relationship between inverse second moment, $\langle H^2\rangle^{-1}$ and inverse central line width, ΔH_0^{-1}, showing clustering of secondary structural motifs. The points for SL-IA$_3$ are circled and emboldened. The shaded points for known structural regions are taken from the literature [1,8–10].

and small RNAs [19,20], correlation times are often <2 ns. This time regime is regarded as the "fast motion" limit for X-band CW EPR nitroxide spectra; where the narrowed line shapes no longer show marked differences via $\langle H^2\rangle^{-1}$ and ΔH_0^{-1} analysis and where extraction of correlation times and models of motion via in-depth simulation procedures is challenging due to the non-descript "isotropic-like" nature of the spectra. A key example where X-band EPR spectra are often in the "fast motion" limit is in SDSL studies of intrinsically disordered proteins (IDPs).

IPDs are defined as "proteins or protein segments of 50 or more residues that lack highly populated secondary and tertiary structure under physiological conditions" [21–27]. These highly dynamic proteins are characteristically either fully unstructured, molten globular, contain flexible linkers between structured domains, or possess separate domains of varying degree of structure or lack of structure. There is significant interest in the structural and dynamic properties of IDPs due to their importance in processes such as transcription and translational regulation and cellular signaling, the details of which have been covered in review articles [24,27].

Here we show that SDSL CW EPR spectroscopy at frequencies higher than X-band, particularly W- and D-band frequencies (95 and 130 GHz; respectively), offers "sweet spots" for studying the "fast motion" dynamical behaviors of IDPs. A multi-frequency (MF) SDSL investigation of IA$_3$, a 68 amino acid IDP known to undergo a dynamic transition from unstructured to α-helical conformation upon interaction with tri-fluoroethanol (TFE) in solution, was performed for two spin labeled (SL)-IA$_3$ constructs in various degrees of induced helical transition. Using a combination of experimental and simulated CW EPR nitroxide spectra, we illustrate the utility in frequencies higher than X-band to resolve "fast motion" dynamics in spin-labeled biological macromolecules.

2. Materials and methods

2.1. Reagents

3-(2-Iodoacetamido)- PROXYL (IAP) spin label was purchased from Sigma Aldrich (St. Louis, MO). Unless otherwise stated, all other reagents were purchased from Fisher Scientific (Pittsburg, PA) and used as received.

2.2. Preparation of SL-IA$_3$

Gene cloning, mutagenesis, expression and purification of IA$_3$ via an *Escherichia coli* system were performed as described previously [12], which is a modified purification scheme from the original protocol [28]. Protein was estimated to be >98% pure by a 16.5% Tris–Tricine SDS–PAGE gel. Proteins containing the cysteine substitutions were spin-labeled with IAP as described previously [12]. Excess spin label was removed by buffer exchanged into 50 mM sodium phosphate, 300 mM sodium chloride, pH 7.4 using a HiPrep 26/10 de-salting column (Amersham, Pittsburg, PA).

2.3. Sample preparation

Samples for EPR experiments were prepared by adding the appropriate volume of TFE to protein stock solutions to generate 15% and 30% TFE concentrations. For X-band studies, two samples were also prepared that contained 30% sucrose, one with 0% TFE, the other with 30% TFE. For all samples an appropriate volume of a 10× phosphate buffer stock (desalting elution buffer described above), was added to adjust final buffer concentration to match original protein buffer ensuring consistent ionic strength of all samples. Protein concentration was approximately 200 μM in each case, except for W-band samples; which were concentrated to nearly 2 mM for adequate signal to noise in EPR experiments.

2.4. Electron paramagnetic resonance (EPR) experiments

CW X-band (9.8 GHz) EPR spectra were collected on a modified Bruker ER200 spectrometer, at 27 °C, unless otherwise noted, as described previously [12]. The samples consisted of ~10 μL of sample solution in flame sealed 0.60 i.d. × 0.84 o.d. capillary tubes (Fiber Optic Center, New Bedford, MA). All X-Band spectra were collected over a 100 Gauss field range.

CW Q-band (35 GHz) EPR spectra were collected on a Bruker E500 spectrometer equipped with an ER 5106 QT-W resonator. Spectra were collected at ambient temperature. Each of the samples consisted of ~2 μL of solution loaded into 0.4 o.d. quartz tubes from Vitrocom (Vitrocom, Mountain Lakes, NJ) that was sealed with X-Sealant. All Q-band spectra were collected over a 120 Gauss field range.

CW W-band (95 GHz) EPR spectra were collected on a Bruker Elexsys 680 spectrometer equipped with a W-band ENDOR resonator at the National High Magnetic Field Lab (NHMFL) in Tallahassee, FL. Temperature was regulated to 27 °C using a CF935 cryostat (Oxford Instruments). Samples were loaded into 0.15 i.d. × 0.25 o.d. suprasil quartz capillary tubes (Vitrocom, Mountain Lakes, NJ) that were sealed with X-Sealant® and placed in a larger quartz tube (0.50 i.d. × 0.90 o.d.) that was then also sealed at one end before inserting into the cavity. All W-Band spectra were collected over a 180 Gauss field range.

Variable parameters for data collection such as the microwave power, field modulation amplitude, modulation frequency, time constant, conversion time, and number of averaged scans were optimized for each collection frequency to maximize signal-to-noise ratio without introducing artificial line shape distortions. The same optimal parameters at each collection frequency were used for each sample. Data were baseline corrected and integral area normalized using LabVIEW software as previously described [12], which was generously provided by Drs. Christian Altenbach and Wayne Hubbell at the University of California, Los Angeles (https://sites.google.com/site/altenbach/labview-programs/epr-programs/multicomponent).

2.5. Spectral simulations

EasySpin software [41,42] was used for simulation of CW EPR spectra at X, Q, W, and D band (9.5, 35, 95, and 130 GHz; respectively). Line shapes were simulated assuming isotropic motion for a nitroxide spin label with various rotational correlation times ranging from 0.1 to 2.1 ns. The simulations were performed using a field sweep width of 100 Gauss for X-band, 130 Gauss for Q-band, 200 Gauss for W-band, and 240 Gauss for D-band each consisting

of 30,000 points with Lorentzian peak-to-peak line broadening of 0.7, 0.9 1.5, and 1.8 Gauss for X-, Q-, W-, and D-band frequencies; respectively. The g-tensor was set to [g_{xx} = 2.0076, g_{yy} = 2.0050, g_{zz} = 2.0023] and the ^{14}N hyperfine coupling tensor was set to [A_{xx} = 7.5, A_{yy} = 5.9, A_{zz} = 35] (Gauss).

3. Results

3.1. X-band CW EPR nitroxide line shapes for SL-IA$_3$

IA_3 is a 68 amino acid protein that is a highly potent inhibitor of the yeast aspartic proteinase, saccharopepsin, also known as YPRA (yeast aspartic proteinase A) [28]. IA_3 is unstructured in solution, but residues 2–32 are known to become α-helical upon binding to YPRA [29] whereas the entire protein can be transitioned to α-helical conformation using TFE [30–33]. The amino acid sequence of IA_3 is shown in Fig. 2A. Single sites were chosen in both the N- and C- termini for cysteine substitution and subsequently labeled with IAP. The details of this procedure have been published previously [12]. The cysteine IAP modification is referred to herein as P1 (Fig 2B). Fig. 2C shows corresponding X-Band CW-EPR spectra for SL-IA_3, where 0% and 30% TFE represent the unstructured and α-helical states; respectively. At X-band frequency, all spectra are relatively narrow, yielding similar empirical line shape parameters that are reflective of high mobility of P1 (Fig. 1). These values fall outside the region typically observed for unstructured regions of large globular or membrane bound proteins indicating that the motions are in the "fast motion" limit of X-band spectra [1,9,10]. Lowering the sample temperature or treating the sample with sucrose can alter protein and P1 mobility. However, as can be seen in Fig. 1, even under these conditions, spectra are narrow and the corresponding empirical line shape parameters still fall outside the range of values traditionally obtained for structured globular or membrane proteins. In addition, these solution modifications represent conditions that are not physiologically relevant. For studies of the biochemical function of IDPs, physiological temperatures without added co-solutes are desired for ascertaining experimental parameters that can be most accurately related to native behaviors.

3.2. Comparing X-, Q- and W-band CW EPR spectra for SL-IA$_3$

A MF approach expands the time scale of motions in IDPs that can be probed using CW EPR to include motions that average to the "fast-limit" at X-band frequencies. These motions produce only intermediate averaging of the nitroxide line shape at higher frequencies [11,34–40]. Fig. 3 shows experimental CW-EPR spectra of SL-IA_3 collected at X-, Q- and W-Band frequencies as a function of induced α-helical structure ranging from the unstructured state (0% TFE) to α-helical state (30% TFE). The X- and Q-band spectra show only slight line shape dispersion over this range of TFE concentration. Moving to W-band, however, clearly resolves the helical transition that occurs when the TFE % (v/v) is increased from 15% to 30%. By comparisons of the W-band spectra with simulations for a range of correlation times <2.1 ns (Fig. 3, discussed in the next section), the transition appears to induce a change in correlation time from ~0.4 ns to ~0.6 ns; which is in the "fast motion" limit for X- and Q-bands. These correlation times were confirmed using LabVIEW software cited in the materials and methods section. These findings suggest that even higher frequencies such as D-band (130 GHz), for example, may be useful for added resolution in the 0% to 15% TFE range. The W-band spectra at 0% and 15% TFE show only a slight change line shape dispersion that may become more evident with the higher frequency.

3.3. Simulations of nitroxide CW EPR line shapes at multiple frequencies

In order to further demonstrate the sensitivity of higher frequency CW EPR to dynamical motions beyond the "fast motion" limit at X-band, we performed spectral simulations using EasySpin [41,42] at X-band (9.5 GHz), Q-band (35 GHz), W-band (95 GHz)

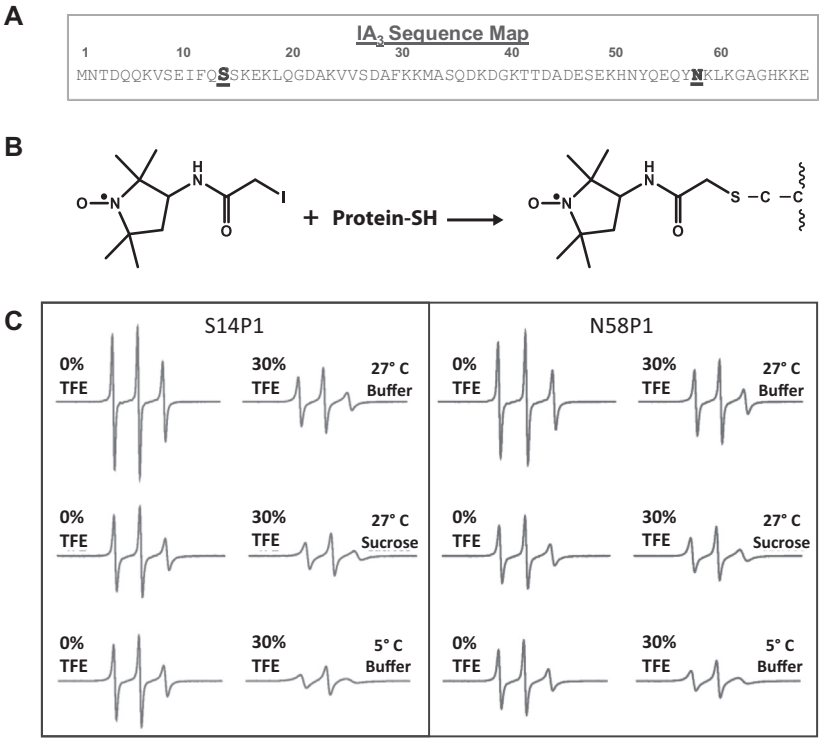

Fig. 2. (A) Amino acid sequence of IA_3 showing sites selected for SDSL. (B) Labeling scheme for IAP. (C) Integral area normalized 100 Gauss X-band CW EPR spectra for SL-IA_3 constructs S14P1 and N58P1 as a function of TFE % (v/v) at either 5 or 27 °C in buffer either with or without added sucrose, as indicated.

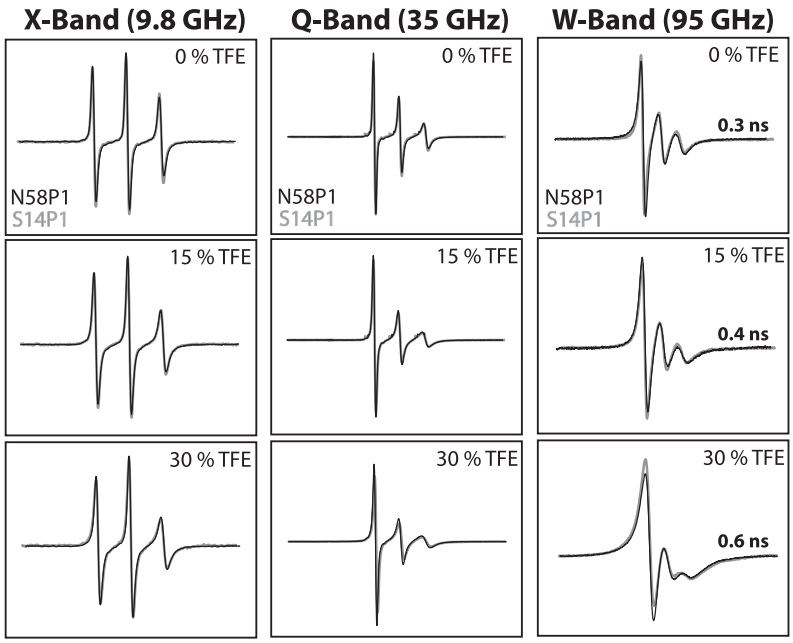

Fig. 3. Comparison of integral area normalized experimental EPR spectra for S14P1 (red) and N58P1 (black) SL-IA$_3$ constructs at X-band (9.8 GHz), Q-band (35 GHz), and W-band (95 GHz). The clear change in line shape between the 15% and 30% TFE samples at W-band indicates a structural transition. The correlation times assigned to the W-band spectra were obtained using LabVIEW software cited in the Section 2.

and D-band (130 GHz) for correlation times of 0.1, 0.3, 0.6, 0.9, 1.5, and 2.1 ns (Fig. 4). For simplicity, simulations were limited to isotropic local motion of the spin label; *i.e.*, orienting potentials and diffusion tensors were not considered. These assumptions reduced the number of parameters necessary to describe the data while allowing for adequate identification of trends in the spectral line shapes. In Fig. 4, the X- and Q-band spectra are in the "fast motion" limit, showing a relative lack of sensitivity to changing correlation times in this range. The W- and D-band spectra, however, show dramatic sensitivity. Changes in correlation times in this range are readily apparent from the spectral line shapes. This illustrates the utility in W- and D-band frequencies for studying dynamic motions in IDPs where correlation times are commonly in the ~0.1–2 ns range [12–18]; corresponding to intermediate motional averaging of the line shapes.

4. Discussion

4.1. X-band SDSL investigations of IDPs

While SDSL EPR at X-band frequencies has been utilized to characterize structure and dynamics in IDPs [1–10,12], the relative insensitivity of X-band CW EPR nitroxide line shapes (insensitivity of $\langle H^2 \rangle$ and ΔH_0) to the fast motions sampled by IDPs have led others to propose an alternative line shape parameter, the ratio of the intensities of the high-field to central field transitions, $h_{(+1)}/h_{(0)}$, as a useful way to monitor changing dynamics in IDPs [13–17]. This methodology has been applied to the N-tail measles protein [13,15], the C-terminal domain of the Henipavirus nucleoprotein [17], and the flexible chloroplast protein CP12 [16], in addition to our own previous studies of IA$_3$ [12], for example. Combined, these studies show that this more non-traditional line shape parameter, $h_{(+1)}/h_{(0)}$, tracks well with correlation times and reflects either induced folding or partner binding. However, these spectra are still reflective of correlation times within the 0.1–2 ns regime, where X-band line shapes are in the "fast motion" limit, which provides limited information regarding uniqueness of motional descriptions via line shape simulations, and where MF and high frequency (HF) CW EPR investigations may provide additional characterization of the dynamics of the unstructured state.

4.2. Multi-frequency and high-frequency EPR

Due to continued technological advances that are providing improved experimental conditions and increased access to instrumentation, applications of HF and MF EPR approaches in biological SL studies are becoming increasingly effective [43]. In particular, a MF approach for studies of dynamics in proteins or nucleic acids allows for global fitting to motional models resulting in lowered ambiguity in fitting/model parameters due to appropriate matching of acquisition frequencies to the time scales corresponding to the different types of dynamic motions (τ_r, τ_B, τ_i, etc.). A comprehensive review of this subject details the benefits and limitations of several theoretical models for approaching SDSL ESR data [44]. It is often pointed out that complex multi-parameter models such as the "slowly relaxing local structure" (SRLS) model or the "microscopic order macroscopic disorder" (MOMD) model [44] can only be reliably addressed with SDSL CW EPR by using a MF approach. For example, in some notable applications of this MF approach to the study of dynamics in T4 lysozyme [38–40,44], it is demonstrated that CW EPR experiments carried out at lower frequencies, such as X-band, suffer from lack of resolution when correlation times approach sub-nanosecond time scales. This is of particular importance for studying IDPs where correlation times typically range from 0.1 to 2 ns [12–18].

The experimental results and simulations presented here demonstrate that with this simple model and the inclusion of W-band and D-band frequencies in CW EPR experiments, we can measure a degree of structural transition in highly dynamic IDPs with a particular sensitivity to "faster" dynamics (0.1–2 ns time regime). Therefore, we suggest these methods for the analysis of structural transitions and motional dynamics in IDPs, where correlation times typically occur in this range [12–18]. We also assert that the benefits of this approach extend beyond IDPs. Dynamic motions in RNAs, for example, have been shown to occur on similar time scales [5,20,45,46].

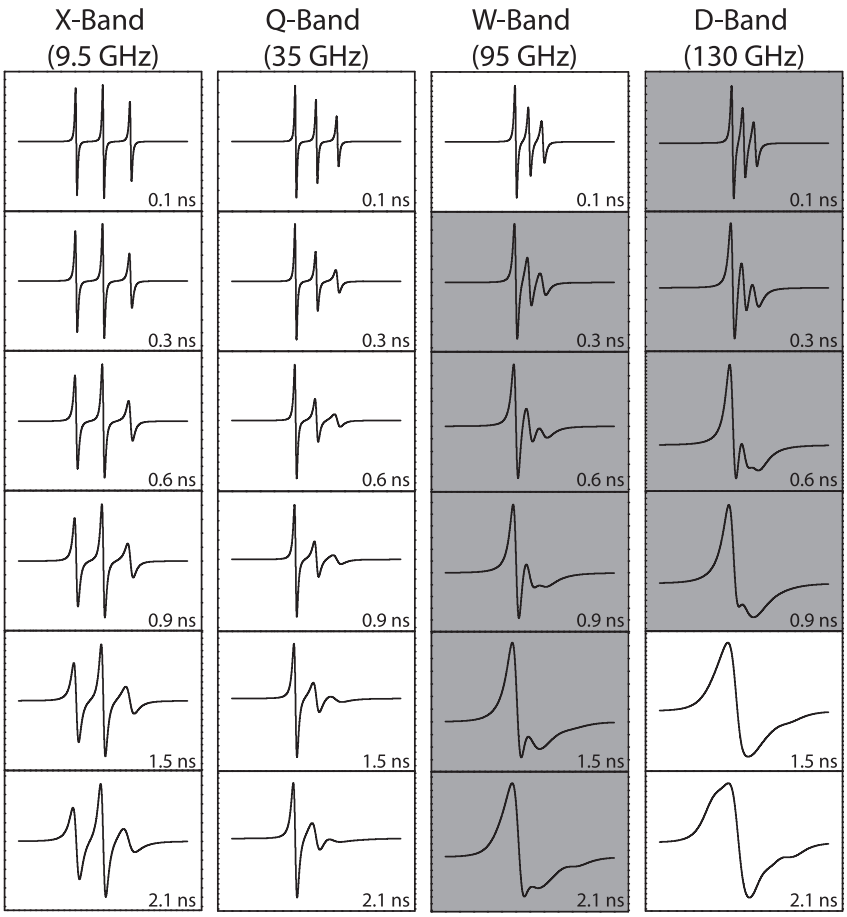

Fig. 4. Comparison of line shapes for spectra simulated at X-, Q-, W-, and D-band frequencies illustrating the relative ranges of correlation times where there is maximum line shape sensitivity. The shaded spectra at W- and D-bands for correlation times from 0.3–2.1 ns and 0.1–0.9 ns respectively, illustrate "sweet spots" between the "fast motion" limit at X- and Q-bands and the "rigid limit" at W- and D-bands.

5. Conclusions

This study highlights the potential of MF and HF CW EPR for characterization of highly dynamic biological macromolecules by providing sensitivity to sub-nanosecond correlation times. With what we have shown, it is apparent that for SDSL EPR studies of structural transitions in IDPs, both W- and D- band frequencies offer enhanced sensitivity to the associated range of correlation times. At these acquisition frequencies, the motional fluctuations are only partially averaging the g and ^{14}N hyperfine tensors of the nitroxide spin label, generating spectra in the intermediate regime. We suggest that the SDSL EPR line shape analyses methods demonstrated here provide an experimental window for studying dynamic motions and structural transitions in IDPs to a much greater level of detail.

Acknowledgments

This work was supported by the National Science Foundation DGE-0802270 (J.M.E.), MCB-0746533 and MCB-1329467 (G.E.F.), and National Institutes of Health S10RR031603 and GM104509 (G.E.F.). We acknowledge the help of Likai Song and Ralph Weber for data collection at W- and Q-band frequencies; respectively, and Stefan Stoll for assistance with EasySpin simulations.

References

[1] G.E. Fanucci, D.S. Cafiso, Recent advances and applications of site-directed spin labeling, Curr. Opin. Struct. Biol. 16 (2006) 644–653.
[2] W.L. Hubbell, C. Altenbach, Investigation of structure and dynamics in membrane proteins using site-directed spin labeling, Curr. Opin. Struct. Biol. 4 (1994) 566–573.
[3] W.L. Hubbell, D.S. Cafiso, C. Altenbach, Identifying conformational changes with site-directed spin labeling, Nat. Struct. Biol. 7 (2000) 735–739.
[4] W.L. Hubbell, A. Gross, R. Langen, M.A. Lietzow, Recent advances in site-directed spin labeling of proteins, Curr. Opin. Struc. Biol. 8 (1998) 649–656.
[5] P. Nguyen, P.Z. Qin, RNA dynamics: perspectives from spin labels, Wiley Interdiscip. Rev. RNA 3 (2012) 62–72.
[6] G.Z. Sowa, P.Z. Qin, Site-directed spin labeling studies on nucleic acid structure and dynamics, Prog. Nucleic Acid Res. Mol. Biol. 82 (2008) 147–197.
[7] L. Columbus, W.L. Hubbell, A new spin on protein dynamics, Trends Biochem. Sci. 27 (2002) 288–295.
[8] H.S. McHaourab, M.A. Lietzow, K. Hideg, W.L. Hubbell, Motion of spin-labeled side chains in T4 lysozyme. Correlation with protein structure and dynamics, Biochemistry 35 (1996) 7692–7704.
[9] M. Kim, G.E. Fanucci, D.S. Cafiso, Substrate-dependent transmembrane signaling in TonB-dependent transporters is not conserved, Proc. Natl. Acad. Sci. U.S.A. 104 (2007) 11975–11980.
[10] J.M. Isas, R. Langen, H.T. Haigler, W.L. Hubbell, Structure and dynamics of a helical hairpin and loop region in annexin 12: a site-directed spin labeling study, Biochemistry 41 (2002) 1464–1473.
[11] D.E. Budil, S. Lee, S. Saxena, J.H. Freed, Nonlinear-least-squares analysis of slow-motion EPR spectra in one and two dimensions using a modified Levenberg–Marquardt algorithm, J. Magn. Reson. 120 (1996) 155–189.
[12] N.L. Pirman, E. Milshteyn, L. Galiano, et al., Characterization of the disordered-to-alpha-helical transition of IA(3) by SDSL–EPR spectroscopy, Protein Sci. 20 (2011) 150–159.
[13] B. Morin, J.M. Bourhis, V. Belle, et al., Assessing induced folding of an intrinsically disordered protein by site-directed spin-labeling electron paramagnetic resonance spectroscopy, J. Phys. Chem. B 110 (2006) 20596–20608.
[14] A. Kavalenka, I. Urbancic, V. Belle, et al., Conformational analysis of the partially disordered measles virus N(TAIL)-XD complex by SDSL EPR spectroscopy, Biophys. J. 98 (2010) 1055–1064.
[15] V. Belle, S. Rouger, S. Costanzo, et al., Mapping alpha-helical induced folding within the intrinsically disordered C-terminal domain of the measles virus

nucleoprotein by site-directed spin-labeling EPR spectroscopy, Proteins-Structure Funct. Bioinformatics 73 (2008) 973–988.
[16] E. Mileo, M. Lorenzi, J. Erales, et al., Dynamics of the intrinsically disordered protein CP12 in its association with GAPDH in the green alga *Chlamydomonas reinhardtii*: a fuzzy complex, Mol. Biosyst. 9 (2013) 2869–2876.
[17] M. Martinho, J. Habchi, Z. El Habre, et al., Assessing induced folding within the intrinsically disordered C-terminal domain of the Henipavirus nucleoproteins by site-directed spin labeling EPR spectroscopy, J. Biomol. Struct. Dyn. 31 (2013) 453–471.
[18] E. Mileo, E. Etienne, M. Martinho, et al., Enlarging the panoply of site-directed spin labeling electron paramagnetic resonance (SDSL–EPR): sensitive and selective spin-labeling of tyrosine using an isoindoline-based nitroxide, Bioconjug. Chem. 24 (2013) 1110–1117.
[19] P.Z. Qin, J. Feigon, W.L. Hubbell, Site-directed spin labeling studies reveal solution conformational changes in a GAAA tetraloop receptor upon Mg(2+)-dependent docking of a GAAA tetraloop, J. Mol. Biol. 351 (2005) 1–8.
[20] P.Z. Qin, J. Iseri, A. Oki, A model system for investigating line shape/structure correlations in RNA site-directed spin labeling, Biochem. Biophys. Res. Commun. 343 (2006) 117–124.
[21] V.N. Uversky, Intrinsically disordered proteins from A to Z, Int. J. Biochem. Cell. Biol. 43 (2011) 1090–1103.
[22] M. Sickmeier, J.A. Hamilton, T. LeGall, et al., DisProt: the database of disordered proteins, Nucleic Acids Res. 35 (2007) D786–D793.
[23] B. He, K. Wang, Y. Liu, et al., Predicting intrinsic disorder in proteins: an overview, Cell Res. 19 (2009) 929–949.
[24] A.K. Dunker, I. Silman, V.N. Uversky, J.L. Sussman, Function and structure of inherently disordered proteins, Curr. Opin. Struct. Biol. 18 (2008) 756–764.
[25] H.J. Dyson, P.E. Wright, Intrinsically unstructured proteins and their functions, Nat. Rev. Mol. Cell. Biol. 6 (2005) 197–208.
[26] H.J. Dyson, P.E. Wright, Coupling of folding and binding for unstructured proteins, Curr. Opin. Struct. Biol. 12 (2002) 54–60.
[27] V.N. Uversky, Natively unfolded proteins: a point where biology waits for physics, Protein Sci. 11 (2002) 739–756.
[28] L.H. Phylip, W.E. Lees, B.G. Brownsey, et al., The potency and specificity of the interaction between the IA3 inhibitor and its target aspartic proteinase from *Saccharomyces cerevisiae*, J. Biol. Chem. 276 (2001) 2023–2030.
[29] M. Li, L.H. Phylip, W.E. Lees, et al., The aspartic proteinase from *Saccharomyces cerevisiae* folds its own inhibitor into a helix, Nat. Struct. Biol. 7 (2000) 113–117.
[30] O.K. Ganesh, T.B. Green, A.S. Edison, S.J. Hagen, Characterizing the residue level folding of the intrinsically unstructured IA3, Biochemistry 45 (2006) 13585–13596.
[31] T.B. Green, O. Ganesh, K. Perry, et al., IA3, an aspartic proteinase inhibitor from *Saccharomyces cerevisiae*, is intrinsically unstructured in solution, Biochemistry 43 (2004) 4071–4081.
[32] R. Narayanan, O.K. Ganesh, A.S. Edison, S.J. Hagen, Kinetics of folding and binding of an intrinsically disordered protein: the inhibitor of yeast aspartic proteinase YPrA, J. Am. Chem. Soc. 130 (2008) 11477–11485.
[33] J. Wang, Y. Wang, X. Chu, et al., Multi-scaled explorations of binding-induced folding of intrinsically disordered protein inhibitor IA3 to its target enzyme, Plos Comput. Biol. 7 (2011) e1001118.
[34] A. Savitsky, M. Kuhn, D. Duche, et al., Spontaneous refolding of the pore-forming colicin A toxin upon membrane association as studied by X-band and W-band high-field electron paramagnetic resonance spectroscopy, J. Phys. Chem. B 108 (2004) 9541–9548.
[35] Y.E. Nesmelov, R.V. Agafonov, A.R. Burr, et al., Structure and dynamics of the force-generating domain of myosin probed by multifrequency electron paramagnetic resonance, Biophys. J. 95 (2008) 247–256.
[36] Y.E. Nesmelov, C.B. Karim, L. Song, et al., Rotational dynamics of phospholamban determined by multifrequency electron paramagnetic resonance, Biophys. J. 93 (2007) 2805–2812.
[37] G.F. White, L. Ottignon, T. Georgiou, et al., Analysis of nitroxide spin label motion in a protein–protein complex using multiple frequency EPR spectroscopy, J. Magn. Reson. 185 (2007) 191–203.
[38] Z.W. Zhang, M.R. Fleissner, D.S. Tipikin, et al., Multifrequency electron spin resonance study of the dynamics of spin labeled T4 lysozyme, J. Phys. Chem. B 114 (2010) 5503–5521.
[39] Z.C. Liang, Y. Lou, J.H. Freed, et al., A multifrequency electron spin resonance study of T4 lysozyme dynamics using the slowly relaxing local structure model, J. Phys. Chem. B 108 (2004) 17649–17659.
[40] J.P. Barnes, Z.C. Liang, H.S. Mchaourab, et al., A multifrequency electron spin resonance study of T4 lysozyme dynamics, Biophys. J. 76 (1999) 3298–3306.
[41] S. Stoll, A. Schweiger, EasySpin, a comprehensive software package for spectral simulation and analysis in EPR, J. Magn. Reson. 178 (2006) 42–55.
[42] S. Stoll, A. Schweiger, EasySpin: simulating cw ESR spectra, Biol. Magn. Reson. 27 (2007) 299–321.
[43] G. Jeschke, Conformational dynamics and distribution of nitroxide spin labels, Prog. Nucl. Mag. Res. Sp. 72 (2013) 42–60.
[44] Z.C. Liang, J.H. Freed, An assessment of the applicability of multifrequency ESR to study the complex dynamics of biomolecules, J. Phys. Chem. B 103 (1999) 6384–6396.
[45] J.M. Esquiaqui, E.M. Sherman, S.A. Ionescu, et al., Characterizing the dynamics of the leader–linker interaction in the glycine riboswitch with site-directed spin labeling, Biochemistry 22 (2014) 3526–3528.
[46] Q.Q. Mao, Y.B. Li, X.Y. Zheng, et al., Up-regulation of E-cadherin by small activating RNA inhibits cell invasion and migration in 5637 human bladder cancer cells, Biochem. Biophys. Res. Commun. 375 (2008) 566–570.